Satellite Magnetic Field Measurements: Applications in Studying the Deep Earth

Catherine G. Constable and Steven C. Constable

Institute of Geophysics and Planetary Physics, Scripps Institution of Oceanography, University of California at San Diego, La Jolla, California

Following a 20 years hiatus, there are several magnetometry satellites in near-Earth orbit providing a global view of the geomagnetic field and how it changes. The measured magnetic field is an admixture of all field sources, among which one must identify the contributions of interest, namely (1) the field generated in Earth's core, and (2) the fields induced in Earth's mantle by external magnetic variations used in studies of electrical conductivity. Models of the core field can be downward continued to the core surface under the assumption that Earth's mantle is a source free region with zero electrical conductivity. Additional assumptions are invoked to estimate the fluid flow at the core surface. New satellite measurements provide an unprecedented view of changes in the core over the past 20 years; further measurements will clarify the temporal spectrum of the secular variation. Secular changes are coupled to changes in length of day, and recent modeling of torsional oscillations in the core can provide an explanation for the abrupt changes in the field known as geomagnetic jerks. Mantle induction studies require a comprehensive approach to magnetic field modeling. Unwanted internal field contributions are removed to yield time series of external variations and their induced counterparts: improved modeling, combined with the increased data accuracy, and longer term magnetic measurements make conductivity studies feasible. One-dimensional global conductivity responses have been estimated under strong assumptions about the structure of the source field. Ongoing improvements to this work will take account of more complicated source-field structure, three-dimensional Earth structure, and spatio-temporal aliasing due to satellite motion. Modeling of three-dimensional near surface conductivity structure, and the use of time-domain rather than frequency-domain techniques to estimate the 3-D Earth response are needed. Progress could be furthered by future magnetometer missions that involve multiple satellite configurations.

EARTH'S MAGNETIC ENVIRONMENT

Earth has its own internally generated magnetic field, the bulk of which arises from a self-sustaining dynamo that operates in the liquid outer part of the core. The magnetic field is a dynamic entity and varies significantly on all temporal and spatial scales. The most dramatic changes are field reversals, which take several thousand years to complete and occur at irregular intervals, typically a few times per million years, although the reversal rate has varied over Earth's history. Time variations arising from the geodynamo induce magnetic fields in Earth's electrically conducting mantle, and the internal field is also responsible for both remanent and induced magnetic field anomalies found in Earth's lithosphere. The internal geo-

The State of the Planet: Frontiers and Challenges in Geophysics
Geophysical Monograph 150, IUGG Volume 19

10.1029/150GM13

magnetic field plays a protective role in shielding the environment from cosmic rays: the magnetic pressure also holds off the solar wind and prevents stripping of Earth's atmosphere. The cold plasma that forms the solar wind contributes to Earth's complicated magnetic environment: the solar wind interacts with the internal field and is the cause of temporal variations on a broad range of time scales in both the external magnetospheric and ionospheric fields and their induced counterparts in Earth's lithosphere and mantle [see *e.g.*, *Campbell*, 1997].

This chapter is concerned with magnetic field measurements made from satellites, what they contribute to our knowledge of the geodynamo, and how they can be used to probe the electrical conductivity of Earth. Compared with the relatively sparse array of a few hundred land-based magnetic observatories, magnetic satellites provide essentially complete coverage of the entire globe. For example, the International Geomagnetic Reference Field (IGRF), the definitive model of Earth's magnetic field, is limited by observatory distribution to spherical harmonic degree and order 13, or about a 3,000 km resolution. Satellite measurements, however, are limited only by the flight altitude, or about 500 km, and models up to degree 60 are possible. Satellites provide continuous measurements during the mission, and although untangling the spatial and temporal variations in the field presents novel challenges, the long period changes in the field that are generated by secular variation in the geodynamo and the shorter period variations that are useful for probing mantle conductivity are both resolved in a unique way. Vector magnetic satellite missions are the best way to study Earth's magnetic field.

The magnetic field has its origin in a number of distinct locations and processes which are defined in Plate 1. The measured field is an admixture of fields from external sources in the magnetosphere and ionosphere, internal sources in the crust, and core, and secondarily induced fields in Earth's electrically conducting ocean, lithosphere, and mantle which arise from primary time varying fields from within the core and external to the Earth. Separating the individual contributions to the magnetic field remains an active area of research. We are concerned with isolating (1) the field generated in Earth's liquid outer core and associated secular variations that provide a view of the workings of the geodynamo, and (2) fields induced in Earth's mantle by large scale external magnetospheric variations; these arise from the interaction of Earth's internal magnetic field with the solar wind and are used in studies of electrical conductivity. Crustal magnetization, itself a major topic of geophysical interest [*Langel and Hinze*, 1998], contributes significantly to the measured field, and must be considered in attempts to isolate the fields in both core and mantle. The rotation of the earth beneath the sun providing a daily heating cycle is evident in the diurnal variation of ionospheric *Sq* currents which can also be used in electrical conductivity studies using ground-based observatory data: however, since they lie below the satellite measuring region we do not consider that application here, but treat them as an unwanted source of noise.

Two simplifying strategies used in geomagnetic studies exploit the fact that individual sources contribute magnetic fields that vary on distinct temporal or spatial scales. It may be possible to isolate a particular part of the magnetic field purely on the basis of how it changes with time. Figure 1 presents an amplitude spectrum of geomagnetic variations as a function of frequency, with annotations indicating the predominant physical processes that contribute at the various timescales. It is clear that the largest variations occur at the very long time scales associated with geomagnetic reversals. It is less than 50 years since the OGO satellites (1965–1971) provided the first high precision global geomagnetic surveys, and the temporal variations that can be measured directly are rather small in comparison with the overall signal. Nevertheless, satellite measurements sample a number of significant processes in the geomagnetic spectrum shown in Figure 1, with frequencies ranging from about 25 Hz to periods of several years. This covers a range of external field phenomena and extends well into the regime of internal field secular variations. One complication is that both solar controlled magnetospheric and core processes contribute to field variations on timescales ranging from several months to at least decades (solar variability certainly occurs at much longer timescales), obviously a unique separation cannot be accomplished just using time variations in the field for a single location.

The second strategy we bring to bear is a spatial separation of contributions to the magnetic field: firstly, according to whether the source lies above or below the region in which measurements are made, and secondly according to spatial scale. To achieve this the usual assumption is to regard the measurement region as being free of magnetic field sources: this is an excellent approximation for ground-based measurements, as the atmosphere beneath the ionosphere is essentially an insulator. In a source free region the static magnetic field, $\vec{B}$, can be represented as the gradient of a scalar potential, Ψ, satisfying Laplace's equation ($\nabla^2\Psi = 0$). The general solution to Laplace's equation yields a spherical harmonic representation for the geomagnetic field that provides a formal separation between internal and external sources, and within each source region decomposes the field according to spherical harmonic degree, l, and order m. The degree and order of a term within the spherical harmonic expansion determines the spatial scale of that contribution to the magnetic field: low degrees correspond to the largest spatial scales, with $l = 1$ being the largest scale dipole part of the field. This representation was used by Gauss in the 19th century to generate a least squares fit to magnetic observatory data and show that by far the largest part of the geo-

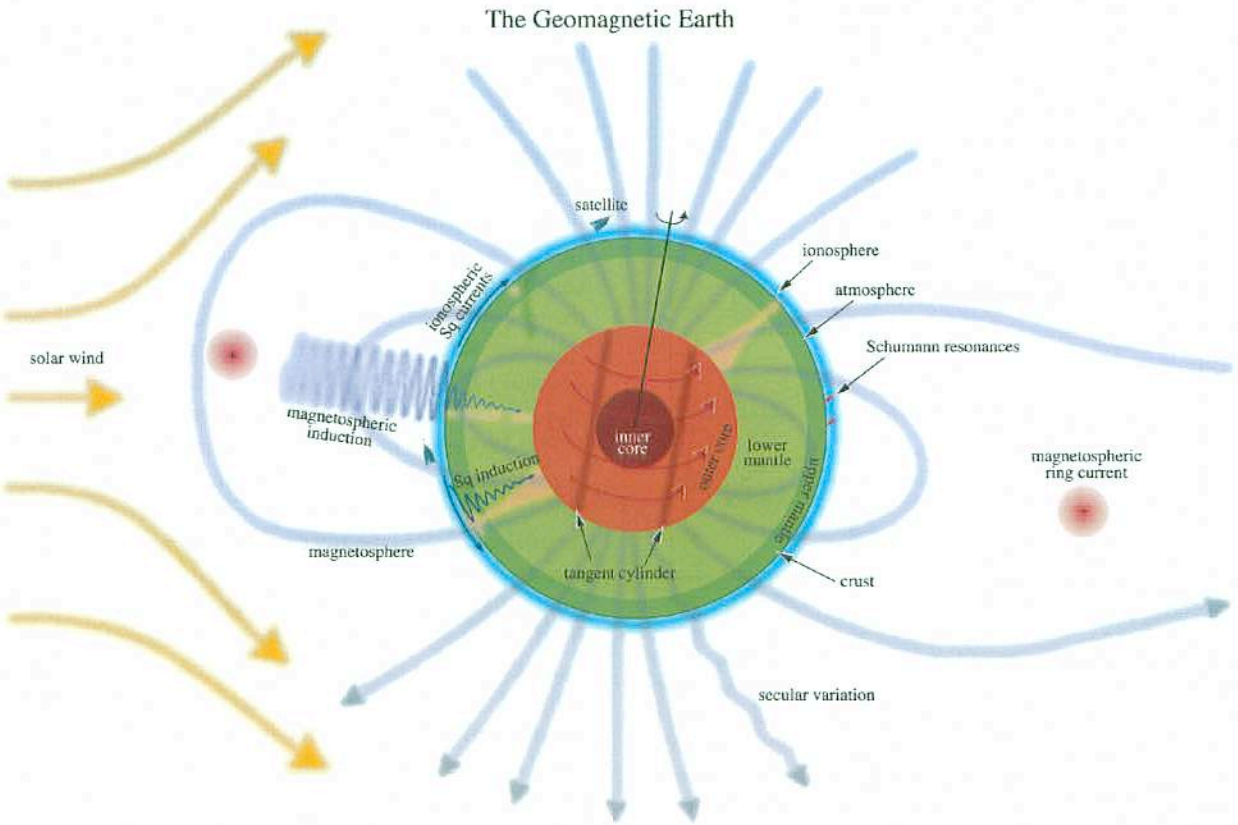

Plate 1. Earth's magnetic field is generated in the liquid **outer core**, where fluid flow is influenced by Earth rotation and the **inner core** geometry (which defines the **tangent cylinder**). Core fluid flow produces a **secular variation** in the magnetic field, which propagates upward through the relatively electrically insulating **mantle** and **crust**. The crust makes a small static contribution to the overall field. Above the insulating **atmosphere** is the electrically conductive **ionosphere**, which supports **Sq currents** as a result of dayside solar heating. Lightning generates high frequency **Schumann resonances** in the Earth/ionsophere cavity. Outside the solid Earth the **magnetosphere**, the manifestation of the core dynamo, is deformed and modulated by the solar wind, compressed on the sunside and elongated on the nightside. At a distance of about 3 earth radii, the **magnetospheric ring current** acts to oppose the main field and is also modulated by solar activity. Magnetic fields generated in the magnetosphere and ionosphere propagate by **induction** into the conductive Earth, providing information on electrical conductivity variations in the crust and mantle. **Magnetic satellites** fly above the ionosphere, but below the magnetospheric induction sources.

magnetic field is of internal origin. Solution of Laplace's equation by least squares estimation or regularized inversion [see for example, *Parker*, 1994] forms the backbone of many magnetic field analyses conducted today. *Langel* [1987] provides a review of the methods used.

The spherical harmonic representation can be used to provide a spatial analog of the amplitude/frequency spectrum of Figure 1. The spatial power spectrum for the magnetic field is usually defined as the average power in $\vec{B}$ at Earth's surface as a function of spherical harmonic degree: spherical harmonic degree plays the role of spatial wavelength, and an approximate length scale is given by $\pi a/l$ with a the radius of the earth. Plate 2 shows the spatial power spectrum for a range of recent models derived from both satellite [CO2, *Holme et al.*, 2003; MF, *Maus et al.*, 2002, 2003; OSVM *Olsen*, 2002; LPPC, *Lowe et al.*, 2001) and aeromagnetic data [KCP, *Korte et al.*, 2002]. Symbols represent spectra calculated from spherical harmonic models as an intermediate step. Curves (KCP and LPPC spectra) are derived from along and cross track power and cross spectra estimated directly from satellite passes or very long-track, high-altitude, aeromagnetic surveys using a technique described by *O'Brien et al.* [1999]. The range of spatial scales represented here is from some 10's of km for the aeromagnetic models to the scale of the Earth for the dipole part of the field. The spatial spectrum makes clear that the degree 1 dipole part of the field is

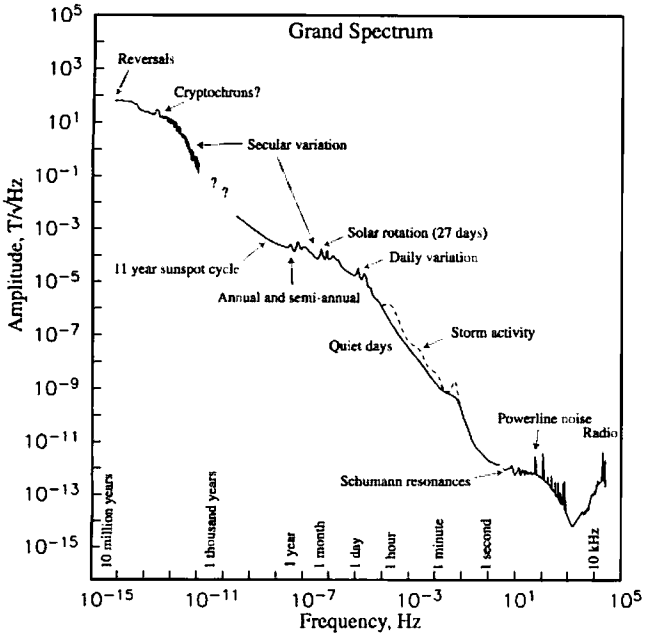

Figure 1. Amplitude spectrum of Earth's geomagnetic field. From 10^{-15} to 10^{-10} Hz, data are from *Constable, Tauxe & Parker* [1998]. Between 10^{-10} and 1 Hz, we have redrawn Figure 3 of *Filloux* [1987]. Above 1 Hz, we use the results of Nichols et al. [1988]. Internal variations associated with motions of the fluid core dominate at periods longer than a few months, culminating in whole reversals of the dipolar part of the field on 10^5 to 10^6 year time scales. The eleven year sunspot cycle, solar rotation, and Earth's orbit modulate the distortions of the field associated with geomagnetic storms, which themselves have energy in the several hour to several second band. Energy at the daily variation and harmonics comes from diurnal heating of the ionosphere. Lightning creates high frequency energy in the Earth/ionosphere cavity, which resonates at 7–8 seconds and harmonics. At the highest frequencies man-made sources dominate—it is unlikely that the natural spectrum abandons its red nature as shown in this figure.

dominant, but there are substantial higher degree contributions. Somewhere between degrees 11 and 15 the contribution of the internal core field is overwhelmed by that of the lithosphere, whose contribution remains relatively flat out to about degree 1000. The slight increase in power at highest degrees for each of the satellite spherical harmonic crustal models is probably an artifact due to measurement and external field noise and the truncation level chosen in least squares spherical harmonic modeling. The KCP and LCCP spectra have had the core field (below degree 13) removed, prior to estimating the crustal power spectra. Also shown on Plate 2 are the power contributions from the large scale degree 1 and 2 static part of the external field, and the power in the core field secular variation in $(nT/yr)^2$ for the year 2000.0 as a function of spherical harmonic degree for the OSVM [*Olsen*, 2002].

The external fields due to the magnetospheric ring current (often referred to as the disturbance storm time, or *Dst*, because large magnetic disturbances are caused by magnetic storms) and *Sq* currents in the ionosphere are the major contributors to short term variations (see Figure 1) although the static part of these fields is not large. Magnetic storms caused by changes in the solar wind can generate rapid changes in these external fields. Short term variations originating in the core are attenuated by their passage through the (slightly) electrically conducting mantle. However, there is overlap in the temporal spectrum of internal and external variations. The shortest term internal variations that have been identified are the sudden changes in $d\vec{B}/dt$, known as geomagnetic jerks [*Courtillot et al.*, 1978], detected in monthly or annual mean observatory records. No jerk has yet been captured in satellite measurements, although there is evidence that jerks recur at approximately decadal intervals [see for example *Mandea et al.*, 2000]. At periods ranging from months to tens of years and longer there are significant changes in both external and internal parts of the field. The 11-year solar cycle variations are a well known example of long period modulations of external field variations. Of course, these external variations induce corresponding internal variations in addition to the changes arising in Earth's core. There are ongoing efforts to model all significant internal and external magnetic field contributions and their time variations using both satellite and observatory data. In the geomagnetic community this approach is known as Comprehensive Magnetic Field Modeling [*Sabaka et al.*, 2002].

MAGNETIC SATELLITE MISSIONS

Magnetic measurements have routinely been carried out on the ground and over the oceans since the 16th century [see *Jackson et al.*, 2000], but it is only since the OGO missions that we have acquired the global view of the geomagnetic field from space. Early magnetometer missions carried scalar magnetometers, but *Backus* [1970] showed that field models derived from fixed altitude intensity data alone are intrinsically non-unique. This led to the development of the first vector magnetic field satellite, known as Magsat, which was active from November 1979 to May 1980. Following Magsat there was a 20 year hiatus in satellite magnetometer missions until the launch of the Danish satellite Ørsted in February 1999. Renewed interest in geomagnetic measurements has led to the promotion of an International Decade of Geopotential Research, and 2 additional satellites are currently mapping the field (CHAMP and Ørsted-2/SAC-C). In contrast to Magsat, which was confined to an 06:00/18:00 local time orbit, Ørsted and CHAMP will sample all local times. Ørsted-2/SAC-C is in a 10:30/22:30 local time orbit. Altitudes range from 400 km (circular) for CHAMP to 650–850 km for Ørsted.

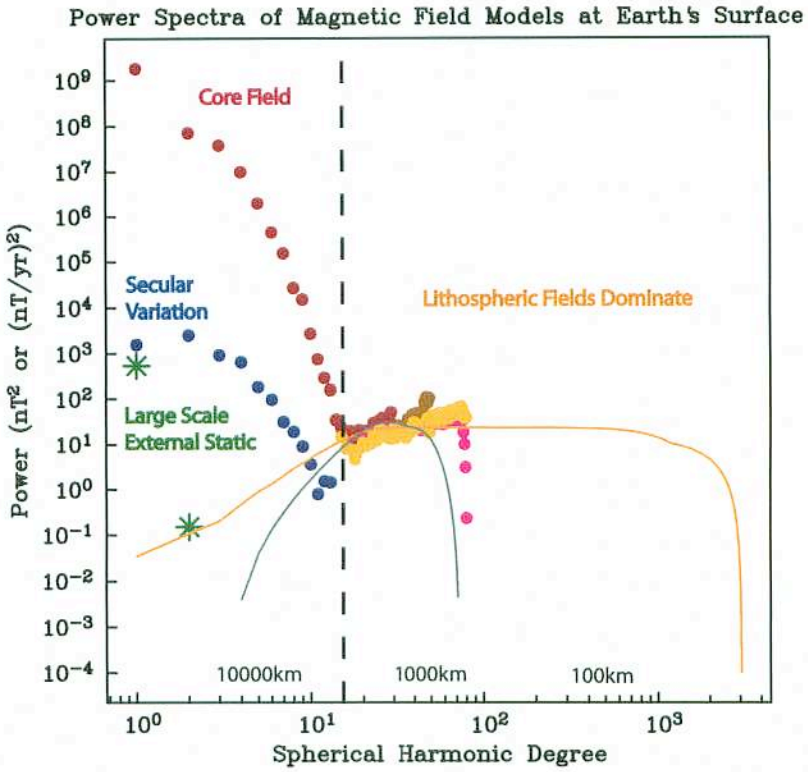

Plate 2. The spherical harmonic power spectrum for the geomagnetic field. For each degree l the power is the average of the square of the magnetic field intensity (or for secular variation, $(d\vec{B}/dt)^2$) over Earth's surface calculated for the designated model. The spherical harmonic degree is a measure of the lengthscale under consideration. CO2+ (brown main field, green external static)is described by *Holme et al.* [2003], OSVM (red main field, blue secular variation) by *Olsen* [2002], MF1 (yellow, crustal) and MF2 (purple, crustal) by *Maus et al.* [2002, 2003], KCP (orange) by *Korte et al.* [2003] and LPPC (gray) by *Lowe et al.*, [2001].

Vector field missions typically consist of a fluxgate magnetometer combined with one or more star cameras to determine attitude of the spacecraft, GPS for positioning, and a scalar magnetometer for calibration of the vector field instrument. Details of the Ørsted satellite are given by *Stauning* [2003] and the instrument calibration is described by *Olsen et al.* [2003a], and for CHAMP by *Reigber et al.* [2002]. The fact that individual magnetic missions now provide several years of continuous field mapping is facilitating exploration of the part of the geomagnetic temporal spectrum where internal and external field variations overlap (Figure 1).

Satellite observations have a number of obvious advantages over measurements made on the ground by observatories or surveys. The number of observatories is limited and they are irregularly spaced over Earth's surface with a bias to coastlines. Observatory measurements are affected by small scale heterogeneity of the lithospheric field resulting in what are known as *observatory crustal biases* [*Langel*, 1987, p.314]; these can contribute several hundreds of nT to the measured signal. In addition to these very localized effects the many observatories located on or near the coast are particularly sensitive to the *coast effect*, a large scale induction influence due to the conductivity contrast between the ocean and the continental crust (see Plate 4(b)). Satellites provide excellent global coverage and the crustal field attenuates rapidly with increasing distance from the source.

On the downside, satellites fly several hundred kilometers above Earth's surface so that the details of the crustal field are difficult to identify. When mapping the core field the crustal contribution is generally treated as noise: however, the spatial averaging inherent in upward continuation to satellite altitude results in crustal errors that are spatially coherent [*Jackson*, 1990;1994], and this must be considered in the data selection and inversion [*Rygaard-Hjalsted et al.*, 1997]. A further complication arises from the fact that the ionospheric field, and the associated *Sq* variations, lie beneath the satellite measurement region, and the measurement region itself is not entirely free of magnetic sources. The *Sq* variations may be dealt with in core modeling by choosing data from magnetically quiet times of day and/or modeling them using observatory data for which they are an

external field. The comprehensive field modeling effort [*Sabaka et al.*, 2002] includes the influence of sources in the measurement region using a technique developed by *Olsen* [1996,1997; *Engels & Olsen*, 1998].

CORE FIELD MODELING USING SATELLITE OBSERVATIONS

As already indicated, core field modeling is usually accomplished by selecting data with minimal external field contributions and solving Laplace's equation for the scalar potential under the assumption that the measurement region is field free. Various data selection criteria are used, ranging from using only night-time data (or, more stringently, data that fall entirely on the shadow side of Earth) to choosing data on the basis of the magnetic indices [*Campbell*, 1997], such as the *Kp* index (usually $Kp \leq 1+$) and the *Dst* index ($\leq \pm 10\ nT$), both of which indicate the strength of external geomagnetic field activity. At high latitudes using only scalar field measurements minimizes the effect of field aligned currents found in the satellite measurement region. An additional selection criterion based on the strength of the dawn-dusk component, $|B_y|$, of the interplanetary magnetic field may also be used to minimize the effect of polar cap ionospheric currents. Recent improvements in internal field modeling have focused on improved corrections for the external field, and the inclusion of higher degree terms for the crustal part: it is impossible to separate the core and crustal contributions unambiguously, but general practice is to attribute at least to degree 11 predominantly to the core. Non-Gaussian data errors are accommodated by using iteratively reweighted least squares with Huber weights to achieve a robust fit [*Olsen*, 2002]. External fields are often modeled using the *Dst* index as a proxy for large scale external fields, and a fixed ratio of 0.27 for the internally induced variations, combined with appropriate terms to accommodate seasonal variations. However, as is well known from conductivity studies, this ratio is actually frequency dependent.

Details for two recent models (OSVM and CO2+) based on Ørsted and CHAMP satellites combined with observatory measurements are supplied by their respective authors [*Olsen*, 2002; *Holme et al.*, 2003). The data used in these models span a significant time interval making it possible to derive a secular variation model in addition to the static main field and low degree external field variations. OSVM is a model for epoch 2000.0 with linear secular variation (SV) in spherical harmonic coefficients up to degree 13, and main field coefficients, representing the core and crust, up to degree 29. CO2+ for epoch 2001.0 uses more data and extends the main field further into the crustal dominated regime, reaching to degree 49. The power spectra for these two models are shown in Plate 2 along with crustal models MF1 and MF2 derived from CHAMP data [Maus et al., 2002, 2003]. The spectrum of secular variations for OSVM indicates that the dominant secular changes are large scale when viewed at Earth's surface, but that the SV spectrum falls off less rapidly with increasing l than that for the main field. The extension of secular variation models to smaller spatial scales with spherical harmonic degree as high as $l = 13$ (probably reliable to $l = 11$ or 12) is one result of these new highly accurate satellite missions: previously SV models have not been computed past degree 8 or 10. The importance of such estimates for our understanding of field behavior is apparent from Figure 1: although the high degree static fields generated in Earth's core are masked by the crustal contribution this is not true for the secular variation (only the induced parts of the crustal field will change in a minor way as a result of SV, the remanent parts remain static). Thus there are greatly improved prospects for studying small scale field variations as more data and better parameterized SV models are developed.

The spherical harmonic representation of the field allows it to be downward or upward continued throughout the region where there are no magnetic sources. The relatively large scale and slow time variations in the core field, combined with the approximation of the mantle as an electrical insulator, make this a good candidate for downward continuation of satellite based models to either Earth's surface or the core-mantle boundary. The neglect of mantle conductivity results in a temporal filtering of the core signal [*Benton & Whaler* 1983; *Backus*, 1983] so that short period field variations will be preferentially attenuated, while the presence of sources in Earth's lithosphere masks the short wavelength time-invariant core field. Downward continuation to the surface of Earth's core provides a completely different view from that at Earth's surface, where higher degree spatial variations are greatly attenuated. This is illustrated in Plate 3 (a) and (b) where the radial component of the core field (up to degree 11) from CO2+ is plotted at Earth's surface, $r = a$, and at the core-mantle boundary, $r = c$. Smaller scale structures dominate the field at $r = c$: the generally low field at Earth's surface over South America and the South Atlantic is resolved into a complex region of magnetic flux with opposite polarity to its surroundings; similarly the north polar region, which has strong negative radial fields at $r = a$, has weak positive flux at the core-mantle boundary. The small-scale details vary somewhat among different models at $r = c$ (downward continuation amplifies the small scale differences in models that are essentially the same at Earth's surface), but the general appearance of such models is similar, with pairs of flux lobes at high latitudes in both northern and southern hemispheres, and a number of significant (and some less significant) regions of magnetic flux that are of opposite polarity to their immediate surroundings.

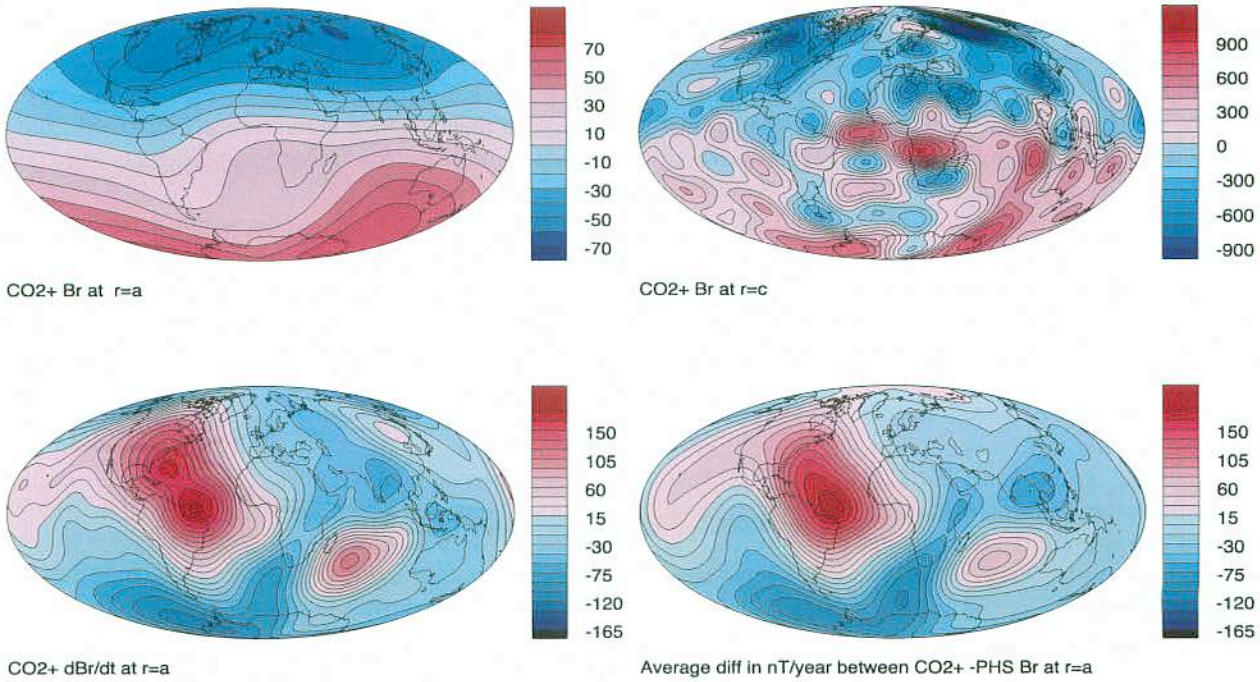

Plate 3. The radial magnetic field for model CO2+ at (a) Earth's surface in 2001.0 and, (b) the core mantle boundary truncated at l = 13. (c) dB_r/dt at Earth's surface for CO2+, the model extends to degree 13 (d) average annual change between CO2+ and PHS, the 1980 field model of *Shure, Parker and Langel* [1985].

Maps of the field at the CMB have been generated from historical data spanning the past 400 years [*Jackson et al.*, 2000], and show the same large scale features, so the important issues concern changes in the field and how these can be interpreted. The lower panels in Plate 3 show dB_r/dt in nT/year at $r = a$, for the CO2+ model in (c), and for comparison the average change in B_r per year calculated from the raw difference between B_r for epochs 1980 and 2001. As might be expected, the CO2+ instantaneous SV differs slightly from the 21 year difference, especially at small scales, reflecting the need for high resolution magnetic satellite data to resolve short temporal variations. On large scales however, there is good agreement between Figs 4(c) and (d). We see that secular variation is largest in the Atlantic hemisphere, especially over the central and southernmost Atlantic, and relatively weak in the Pacific hemisphere. These changes reflect the well-known recent decrease in the dipole moment (at a rate of a few percent/century), but the largest changes are currently in the quadrupole part of the field as seen in the SV spectrum for OSVM in Plate 2 (higher degree variations also contribute). The analog for Plate 3(d) at the CMB would have a great deal of small scale structure that has been amplified by the downward continuation. *Hulot et al.* [2002] computed these changes for an epoch 2000 model primarily based on Ørsted data and note that the changes remain smaller beneath the Pacific, but can be as large as several tens of percent of the field at polar latitudes and below southern Africa. Some of these changes are certainly robust, but there remains the possibility of residual contamination by external fields in the polar regions. The relatively low magnetic field strength beneath the South Atlantic is of considerable interest for two reasons: satellites flying in this region are exposed to increased risk of radiation damage because of the diminished protection associated with weak fields; the rapid field changes in this region suggest the possibility of relatively short term secular variation processes that may involve flux expulsion and ohmic dissipation in the core.

Magnetic field models can also provide dynamical information, and are used to infer the fluid flow at the surface of the core, generally under the additional assumption that the frozen-flux approximation holds: this neglects the effects of electrical diffusion in core field motions and implies that magnetic field lines are locked to the fluid motion. Two components of velocity must be deduced, making such inversions fundamentally non-unique; this dilemma is resolved by imposing further physical constraints on the flow. *Bloxham & Jackson* [1991] provide a review of various options, which include supposing that the flow is steady over time, that it is toroidal (no upwelling or downwelling) or tangentially geostrophic (the horizontal component of the Coriolis force is mainly balanced by the dynamical pressure gradient). The various means of resolving the non-uniqueness result in very similar flows, which may

be a consequence of the fact that they all implicitly assume that the flow is large scale. Independent evidence of the validity of such inversions is supplied by the fact that core surface flows can be used to predict length of day variations on decadal time scales when angular momentum exchanges between core and mantle are taken into account [*Jault et al.*, 1988; *Jackson et al.*, 1993]. The core angular momentum can be calculated from the top of core flow, because the flow in the outer fluid core on decadal time scales is dominated by torsional oscillations. These are simple oscillatory flows that describe differential rigid rotations about the rotation axis of coaxial cylinders (like the inner core tangent cylinder in Plate 1) and for which the magnetic field supplies the restoring force. Torsional oscillations are expected from theory and found in simulated dynamos and real observations. *Bloxham et al.* [2002] have shown that the combination of steady core flow with torsional oscillations can explain the features occurring at roughly decadal intervals (in 1969, 1978, 1991, and 1999) that have been interpreted as geomagnetic jerks.

A recent example of such a core flow is given by *Hulot et al.* [2002], who have calculated the tangentially geostrophic flow that can account for the main field changes they observe between 1980 and 2000. They find a mainly westward axisymmetric flow with some vortices embedded in it. The axisymmetric flow is also symmetric about the equator. Strong polar vortices show westward flow inside the tangent cylinder, an imaginary region outlined by a cylinder parallel to the rotation axis and tangent to the solid inner core. Prograde vortices do exist in some regions. *Hulot et al.* [2002] note that in numerical dynamo models retrograde vortices are associated with upwelling flows and prograde vortices with downwelling. Upwelling flows tend to expel field of reverse polarity (compared with the dipole field) from within the core. However, considerable caution is needed in transferring this interpretation to Earth's field because of the way in which the inherent nonuniqueness is resolved in flow modeling. Under the tangential geostrophic assumption, upwelling or down-welling must occur at the edge of vortices, not the center as seen in numerical simulations. Toroidal flows suffer from a similar lack of realism in that there can be no upward or downward motions in the fluid: nevertheless either kind of flow model can fit the observations. The fact that these kinds of flows satisfy the geomagnetic observations is a start, but it does not guarantee that they accurately reflect the details of what is going on in the core.

INDUCTION STUDIES USING SATELLITE OBSERVATIONS

Induction studies using satellite magnetic measurements rely on the technique known as geomagnetic depth sounding or GDS [*Parkinson*, 1983]. The magnetic field response induced by externally generated field variations follows Faraday's law, and depends on the electrical conductivity in the crust and mantle which in turn reflects the composition, the presence of phase transitions, mantle temperature, and the influence of volatiles and trace materials [*Xu et al.*, 2000]. The depth of penetration into the mantle depends on the frequency content of the time-varying fields and the conductivity of the medium and is characterized by the electromagnetic skin depth, the length scale of exponential decay into Earth. Estimates of the frequency domain transfer function between external and internal fields are the usual data which are interpreted to provide estimates of electrical conductivity as a function of depth. This has proved quite successful in interpreting observations on Earth's surface, which allows the collection of time series of observations at fixed locations [*e.g.*, *Banks*, 1969; *Schultz & Larsen*, 1987; *Roberts*, 1984; *Olsen*, 1998, 1999a; *Constable*, 1993], from which the GDS method is usually used to provide locally one-dimensional (1-D) transfer functions. In principle, such transfer functions can be extended to interpret 3-D variations in electrical conductivity with depth, as well as to accommodate arbitrarily complicated source field structure. In practice these extensions are rarely attempted at a global scale, although differences in the 1-D structure inferred at different locations have been remarked on [*Schultz & Larsen*, 1990; *Weiss & Everett*, 1998]. Recently, substantial progress has been made in forward modeling of 3-D conductivity variations [*Kuvshinov et al.* 1999, 2002b; *Everett & Schultz*, 1996; *Martinec*, 1999; *Uyeshima & Schultz*, 2000]. However, the situation is substantially more complicated for satellite observations than for those on the ground, because the satellite motion results in aliasing of spatial and temporal field variations. In this section we discuss recent progress in using satellite observations to infer 1-D electrical conductivity structure in the mantle and prospects for extending this effort to recover 3-D structures.

1-Dimensional Conductivity Studies

Unlike the situation described in modeling the corefield, in induction studies one is interested in only a small fraction of the signal, typically some tens of nT compared with an average surface field of 45 μT. The first task is to separate some part of the external field variations along with its induced counterpart from the much larger signal generated in Earth's core and the smaller crustal contributions. In ground-based GDS studies the *Sq* ionospheric signal is an external source field and can be used for induction studies, but the ionospheric currents lie below the satellite orbit: thus they are an additional source of noise that must considered in isolating the Dst field variations associated with the magnetospheric ring

current. *Tarits & Grammatica* [2000] have shown that the ionospheric contributions at 400 km can range from 2–4 nT depending on the local time. *Olsen* [1999b] reviews early attempts to use satellite observations for induction studies, which mainly relied on the removal of the core field contribution and its secular variation before analysing the residual signal. More recent induction studies [*Constable & Constable*, 2003; *Korte et al.*, 2003; *Olsen et al.*, 2003] make use of the Comprehensive Magnetic Field Model developed by *Sabaka et al.* [2002], which allows the removal of core and crustal contributions along with an estimate of the quiet time ionospheric *Sq* variations. This provides a significantly better estimate of the signal due to Dst variations in the ring current, although residual *Sq* contamination remains a problem at periods close to 1 day and its harmonics. The spatial structure of the ring current variations is usually approximated by an axial external dipole field configuration in geomagnetic coordinates: these are geocentric coordinates with the z-axis aligned with that of the dipolar part of the internal field: for the CO2+ model the northern end of this axis cuts the Earth's surface at colatitude 10.4°, longitude 288.4°. The simple large scale structure provides a reasonable approximation at geomagnetic latitudes lower than 50°, above this there is substantial contamination by currents in the auroral regions. The size of the auroral signal and attempts to model the current systems that generate it are also discussed by *Fujii & Schultz* [2002] in the context of analysing observatory data.

Once the *Dst* signal has been separated from the bulk of the magnetic signal, one is left with an almost continuous series of vector field measurements in time and space. For each satellite pass (between ± 50° geomagnetic latitude) one can estimate the internal, i_1^0, and external, e_1^0, axial dipole field contributions, thereby producing time series of $i_1^0(t)$ and $e_1^0(t)$ sampled at approximately hourly intervals, the exact interval depending on the satellite orbit. The sum of these times series can be compared directly with the *Dst* index computed from ground observatories. Good agreement between the two [*Constable & Constable*, 2003] indicates that the methodology is robust.

Once the time series $i_1^0(t)$ and $e_1^0(t)$ are obtained the geomagnetic deep sounding method is used to find an electrical impedance response for Earth as a function of frequency. The transfer function,

$$Q_1^0(f) = i_1^0(f)/e_1^0(f)$$

or a transformed variant of it to a complex admittance function [*Weidelt*, 1972], can then be inverted to determine a one-dimensional conductivity profile in the crust and mantle. Figure 2 (inset) shows the admittance function estimates for the Magsat data derived by *Constable & Constable* [2004]. The solid and dashed curves in the inset show the predictions from the 1-D conductivity models plotted in the main part of the figure. As is generally the case in such inversion problems the best-fitting 1-D conductivity profile (derived using *Parker & Whaler's* [1981] D+ inversion algorithm) is unphysical, consisting of 4 delta-functions of conductivity in an insulating half-space. A more realistic conductivity profile with rms misfit of 1.15 (cf 0.95 for the D+ model) is found using regularized inversion, and indicated by the dashed curves: the smoothest model in the sense of minimum first derivative in log conductivity is obtained using a spherical earth variant of the Occam algorithm of *Constable et al.* [1987]. As in the real Earth the model is assumed to have a highly conducting core at a depth of 2886 km. The response functions in Figure 2 are in agreement with estimates obtained by others for Magsat (see also *Olsen et al.* [2003] who attempt the first such analysis using Ørsted data), but have been extended in frequency range at both the high and low ends relative to earlier Magsat analyses by *Olsen* [1999]. This is possible because of improvements in ionospheric field modeling and data processing at high frequencies, and the use of multitaper cross-spectral analyses [*Riedel & Siderenko*, 1995] as opposed to spectral techniques that use section averaging at low frequency.

Inversions of the data in Figure 2 demonstrate that the electromagnetic responses are sensitive to conductivities as shallow as the oceans. The D+ algorithm recovers a surface conductance of 8300 S corresponding nicely with an average ocean conductivity of 3 S/m and 2770 m depth. The regularized model also requires this enhanced near-surface conductivity, a feature not usually recovered from observatory analyses because they are all on land. The upper mantle is relatively uniform in conductivity at around 0.01 S/m which corresponds to that of dry olivine at about 1500° C [*Constable et al.*, 1992]. There is little evidence for a large conductivity increase in the transition zone, but a jump to about 2 S/m occurs at about 700 km depth. This feature has been reported in many conductivity studies and is believed to be associated with the phase transition from garnet and olivine spinel above 670 km to magnesiowüstite and silicate pervoskite at greater depth [e.g., *Xu et al.*, 2000]. A feature in Figure 2 not widely reported in other studies is the further increase at about 1300 km. It is generated by the small imaginary component in the admittance function at long period. This is also observed in a small number of observatory admittance functions (Honolulu is one example, *Schultz & Larsen*, [1987]), which are less representative in their sampling than the satellite. It will be of some interest to see whether this result is confirmed by the newer satellite studies which can deliver longer times series than Magsat. One difficulty that arises is in reliably separating the long period externally induced signal from that induced in the mantle by the shortest period variations arising in the core.

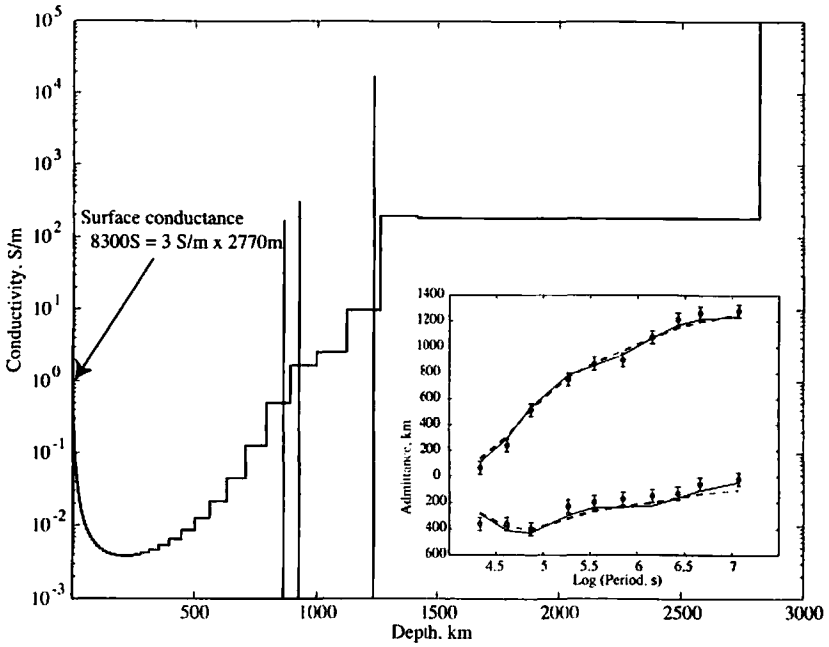

Figure 2. Radially averaged electrical conductivity structure of Earth, from *Constable & Constable's* [2004] treatment of magnetic satellite data. Two models are shown: The vertical bars are a representation of the least squares best fitting model, which is composed of delta functions of conductivity in an otherwise insulating sphere, and includes a surface conductance which nicely agrees with a globally averaged ocean. The inset shows the data (symbols) with the response of this model (solid lines). The stepped conductivity model shows individual layers in a regularized inversion which does not fit the data quite as well (broken lines in inset) but is more realistic. The model is dominated by the conductivity of the surface oceans and deep mantle.

Towards 3-Dimensional Conductivity Studies

The surface conductance recovered from the 1-D conductivity modeling indicates the powerful influence of the oceans and near surface layer in the induction problem. This may mask any interesting 3-D conductivity structures in the mantle, unless its influence can be adequately accounted for and removed. There are at present two approaches to studying the importance of 3-D structures in satellite observations; both rely on time-domain rather than frequency domain analyses, because of the spatio-temporal aliasing that is introduced in the 3-D problem by the satellite's motion. The first approach, adopted by Constable & Constable [2003], is purely qualitative. They suppose that the ratio of $i_1^0(t)/e_1^0(t)$ represents a kind of global time domain response. The normalization of the induced field by the primary field accounts for variations in magnetospheric activity, but since this response can be calculated for a very large number of times and locations the average values in spatial bins of dimension a few degrees can be used to study geographic variations in Earth's electrical response. A further normalization by $\sqrt{1+3\cos^2\theta}$ removes the dependence of the induced dipole field on magnetic colatitude. Plate 4(a) shows the induced magnetic field in Earth as inferred from a stack of over 5000 passes of Magsat data. As might be anticipated the induced fields are systematically lower over continental areas and higher over the more conductive oceanic regions, although this is not the only signal present.

The second approach is illustrated in Plate 4(b) which shows a global model of near-surface conductance constructed from *a priori* knowledge of seawater, and sediment conductivity and thickness [after *Everett et al.*, 2003]. Such models provide a means of undertaking a more systematic analysis of the effects of near-surface heterogeneity in conductivity on the satellite signal. Several forward modeling algorithms now exist [*Kuvshinov et al.*, 2002a,b; *Hamano*, 2002; *Velimsky et al.*, 2003] that allow the prediction of the time domain response of a 3-D earth to a specified primary forcing field. If the appropriate forcing functions can be supplied then in principle these provide a means of stripping out near-surface effects so that underlying variations in mantle conductivity can be studied. One clear result of these studies is that there are major problems associated with interpreting data from discrete observatory locations that are often situated near coastlines [*Kuvshinov et al.*, 2002a].

CONCLUSIONS

We conclude by noting that the burgeoning number of satellite observations are fostering new studies of Earth's core and

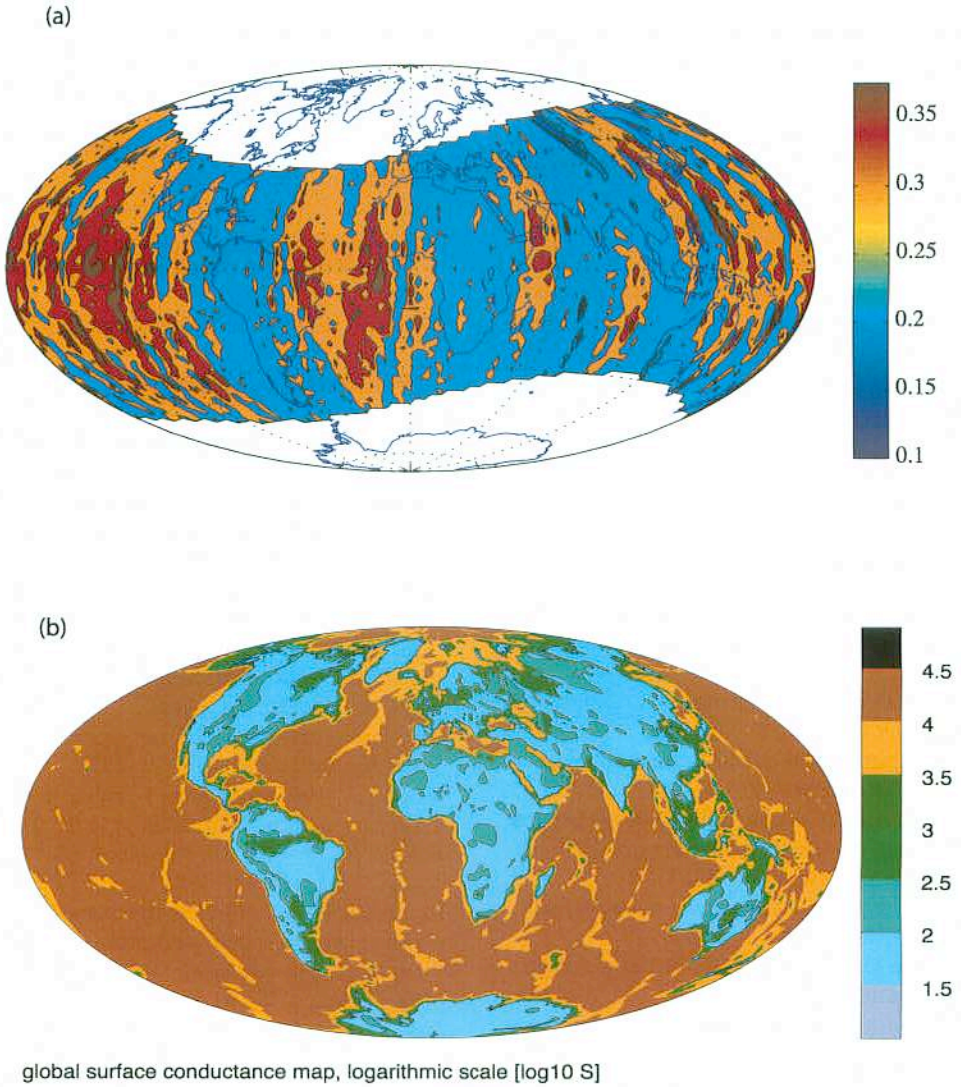

Plate 4. a) The induced internal field normalized by $e_1^0\sqrt{1+3cos^2\theta}$ and averaged in 2 × 3° bins. See text for details (b) Global surface conductance model of *Everett et al.* [2003].

mantle. Observatory estimates of Earth's electrical impedance have been extended spatially and in frequency, and there are good prospects for continued improvement. Inversions demonstrate that the responses are sensitive to conductivities as shallow as the oceans, and we can recover the ocean conductance. Upper mantle conductivity is consistent with hot, dry olivine, and there is little evidence for a large increase in conductivity in the transition zone. The longest period response function estimates probe the lowermost mantle, where satellite responses suggest a substantially more conductive region than is obtained from the average of observatory responses. Electrical conductivity measurements have the potential to play an important role in constraining phase, composition, and temperature variations in the deep mantle, complementing the information garnered from studies that rely on seismic tomography, mineral physics and geochemical arguments. Further investigations of deep mantle structure require longer satellite records and better processing of internal/external field separations.

The 3-D induction problem is most easily tackled in the time domain for satellite data. By stacking the induced field we can get an image of 3-D structure, revealing increased induction over the oceans and smaller induced fields beneath the continents. Forward modeling algorithms exist that allow predictions of the signals expected at the satellite; current limitations are in understanding the spatio-temporal character of the external field variations. More progress can be expected in this area as better analysis tools are developed

and long time series of data become available from multiple satellite configurations like the proposed European SWARM mission.

In the area of core-field modeling the greatest improvements have been in the area of secular variation modeling and the detection of decadal scale field changes. Continued monitoring of the field for a number of years is likely to capture global records of a magnetic jerk as it is occurring, with the possibility of substantial insight into the physical origin of this phenomenon. Other applications of magnetic satellite data include detection of tidal signals from motions in the ocean and using magnetic field measurements to map ocean currents [*Tyler et al.*, 2003].

Acknowledgments. This work was supported by NSF grants EAR-0112290 and EAR-0087391

REFERENCES

Backus, G. E., 1970. Non-uniqueness of the external geomagnetic field determined by surface intensity data. *J. Geophys. Res.*, **A75**, 6339–6341.

Backus, G. E., 1983. Application of mantle filter theory to the magnetic jerk of 1969. *Geophys. J.R. astr. Soc.*, **74**, 713–746.

Banks, R. J., 1969. Geomagnetic variations and the conductivity of the upper mantle. *Geophys. J.R. astr. Soc.*, **17**, 457–487.

Benton, E R & Whaler, K A. 1983. Rapid diffusion of the poloidal geomagnetic field through the weakly conducting mantle: A perturbation solution. *Geophys. J. R. astr. Soc.*, **75**, 77–100.

Bloxham, J. & A. Jackson, 1991. Fluid flow near the surface of Earth's outer core. *Rev. Geophys.*, **29**, 97–120.

Bloxham, J., S. Zatman, & M. Dumberry, 2002. The origin of geomagnetic jerks. *Nature*, **420**, 65–68.

Campbell, W. H., 1997. *Introduction to Geomagnetic Fields*. Cambridge University Press.

Constable, C. G., L. Tauxe, & R. L. Parker, 1998. Analysis of 11 Myr of geomagnetic intensity variation. *J. Geophys. Res.*, **103**, 17,735–17,748.

Constable, S. C., 1993. Constraints on mantle electrical conductivity from field and laboratory measurements. *J. Geomagn. Geoelectr.*, **45**, 707–728.

Constable, S. C. and C. G. Constable, 2004. Observing geomagnetic induction in magnetic satellite measurements & associated implications for mantle conductivity. *Geochem. Geophys. Geosyst.*, **5(1)**, doi:10.1029/2003GC000634.

Constable, S. C., Parker, R. L., and Constable, C. G., 1987. Occam's Inversion: a practical algorithm for generating smooth models from EM sounding data. *Geophysics*, **52**, 289–300.

Constable, S. C., Shankland, T. J. and Duba, A., 1992. The electrical conductivity of an isotropic olivine mantle. *J. Geophys. Res.*, **97**, 3397–3404.

Courtillot, V., J. Ducruix, & J.-L. Le Mouël, 1978. Sur une accélération récente de la variation séculaire du champ magnétique terrestre. *C. R. Acad. Sci D*, **287**, 1095–1098.

Engels, Uta & Nils Olsen, 1998. Computation of magnetic fields within source regions of ionospheric and magnetospheric currents. *J. Atm. Solar-Terr. Phys.*, **60**, 1585–1592.

Everett, M. E., S. C. Constable, & C. G. Constable, 2003. Effects of near-surface conductance on global satellite induction responses. *Geophys. J. Int.*, **153**, 277–286.

Everett, M. E. & A. Schultz, 1996. Geomagnetic induction in a heterogeneous sphere: azimuthally symmetric test computations and the response of an undulating 660 km discontinuity. *J. Geophys. Res.*, **101**, 2765–2783.

Filloux, J. H., 1987. Instrumentation and experimental methods for oceanic studies. In *"Geomagnetism"*, ed. J. A. Jacobs. Academic Press, London, pp. 143–248.

Fujii, I., & A. Schultz, 2002. The 3-D electromagnetic response of the Earth to ring current and auroral excitation. *Geophys. J. Int.*, **151**, 689–709.

Hamano, Y., 2002. A new time-domain approach for the electromagnetic induction problem in a three-dimensional heterogeneous earth. *Geophys. J. Int.*, **150**, 753–769.

Holme, R., N. Olsen, M. Rother, & H. Lühr, 2003. CO2—A CHAMP magnetic field model. In *"First CHAMP Mission Results for Gravity, Magnetic and Atmospheric Studies"*, ed. Ch. Reigber, H. Luehr and P. Schwintzer, Springer-Verlag Berlin, pp. 220–225.

Hulot, G., C. Eymin, B. Langlais, M. Mandea & N. Olsen, 2002. Small-scale structure of the geodynamo inferred from Ørsted and Magsat satellite data. *Nature*, **416**, 620–623.

Jackson, A., 1990. Accounting for crustal magnetization in models of the core magnetic field. *Geophys. J. Int.*, **103**, 657–674.

Jackson, A., 1994. Statistical treatment of crustal magnetization. *Geophys. J. Int.*, **119**, 991–998.

Jackson, A. *et al.*, 1993. Time-dependent flow at the core surface and conservation of angular momentum in the coupled core-mantle system. *Dynamics of Earth's Deep Interior and Earth Rotation*, **Vol. 72**, 97–108.

Jackson, A., A. R. T. Jonkers, M. Walker, 2000. Four centuries of geomagnetic secular variation from historical. *Phil. Trans. R. Soc. Lond.*, **A359**, 957–990.

Jault D., Gire C., and Le Moul J.-L., 1988. Westward drift, core motions and exchanges of angular momentum between core and mantle. *Nature*, **333**, 353–356.

Korte, M., C. Constable, R. L. Parker, 2002. Revised magnetic power spectrum of the oceanic crust. *J. Geophys. Res.*, **107**, 2205, doi:10.1029/2001JB001389.

Korte, M., Constable, S., & Constable, C., 2003. Separation of external magnetic signal for induction studies. In *"First CHAMP Mission Results for Gravity, Magnetic and Atmospheric Studies"*, ed. Ch. Reigber, H. Luehr and P. Schwintzer, Springer-Verlag Berlin, pp. 315–320.

Kuvshinov A.V., N. Olsen, D. B. Avdeev & O. V. Pankratov, 2002a. Electromagnetic induction in the oceans and the anomalous behaviour of coastal C-responses for periods up to 20 days. *Geophys. Res. Lett.*, **29**, 2001GL0144.

Kuvshinov A.V., D. B. Avdeev, O. V. Pankratov, S. A. Golyshev, & N. Olsen, 2002b. Modelling electromagnetic fields in 3-D spherical earth using fast integral equation approach. In *" 3-D Electromag-*

netics", ed. M. S. Zhdanov and P. E. Wannamaker, Elsevier, Holland, pp. .

Kuvshinov A.V., D. B. Avdeev, & O. V. Pankratov, 1999. Global induction by *Sq* and *Dst* sources in the presence of oceans: bimodal solutions for non-uniform spherical surface shells above radially symmetric earth models in comparison to observations. *Geophys. J. Int.*, **137**, 630–650.

Langel, R. A., 1987. The Main Field. In *"Geomagnetism"*, ed. Jacobs, J. A., Academic Press, Orlando, Fla., pp. 249–512.

Langel, R. A., and Hinze, W. J., 1998. *The Magnetic Field of the Earth's Lithosphere: the Satellite Perspective*. Cambridge University Press.

Lowe, D. A. J., R. L. Parker, M. E. Purucker, & C. G. Constable, 2001. Estimating the crustal power spectrum from vector Magsat data. *J. Geophys. Res.*, **106**, 8589–8598.

Mandea, M., E. Bellanger & Jean-Louis Le Mouël, 2002. A geomagnetic jerk for the end of the 20th century?. *Earth Planet. Sci. Lett.*, **183**, 369–373.

Martinec, Z., 1999. Spectral finite-element approach to three-dimensional electromagnetic induction in a spherical Earth. *Geophys. J. Int.*, 136, 229–250.

Maus, S., K. M. Rother, H. Lühr, N. Olsen & V. Haak, 2002. First scalar magnetic anomaly map from CHAMP satellite data indicates weak lithospheric field. *Geophys. Res. Lett.*, **29**, 10.1029/2001GL013685.

Maus, S., K. Hemant, M. Rother, & H. Lühr, 2003. Mapping the lithospheric magnetic field from CHAMP scalar and vector magnetic data. In *"First CHAMP Mission Results for Gravity, Magnetic and Atmospheric Studies"*, ed. C. Reigber, H. Lühr, P. Schwinzer, Springer-Verlag, Berlin, pp. 269–274.

Nichols, E. A., Morrison, H. F., Clarke, J., 1988. Signals and noise in measurements of low-frequency geomagnetic fields. *J. Geophys. Res.*, **93**, 13743–13754 .

O'Brien, M. S., R. L. Parker, & C. G. Constable, 1999. The magnetic power spectrum of the ocean crust on large scales. *J. Geophys. Res.*, **104**, 29,189–29,202.

Olsen, N., 1997. Ionospheric F-Region Currents at Middle and Low Latitudes Estimated From MAGSAT Data. *J. Geophys. Res.*, **102 (A3)**, 4563–4576.

Olsen, N., 1996. A new tool for determining ionospheric currents from magnetic satellite data. *Geophys. Res. Lett.*, **23**, 3635–3638.

Olsen, N., 1998. The electrical conductivity of the mantle beneath Europe derived from C-Responses from 3 h to 720 h. *Geophys. J. Int.*, **133**, 298-308.

Olsen, N., 1999a. Long period (30 days–1 year) electromagnetic sounding and the electrical conductivity of the Mantle beneath Europe. *Geophys. J. Int.*, **138**, 179–187.

Olsen, N., 1999b. Induction Studies With Satellite Data. *Surveys in Geophysics*, **20**, 309–340.

Olsen, N., L. Tøffner-Clausen, T. J. Sabaka, P. Brauer, J. M. G. Merayo, J. L. Jørgensen, J.-M. Lger, O. V. Nielsen, F. Primdahl & T. Risbo, 2003a. Calibration of the Ørsted Vector Magnetometer. *Earth, Planets and Space*, **55**, 11–18.

Olsen, N., S. Vennerstrøm and E. Friis-Christensen, 2003b. Monitoring magnetospheric contributions using ground-based and satellite magnetic data. In *"First CHAMP Mission Results for Gravity, Magnetic and Atmospheric Studies"*, ed. Ch. Reigber, H. Luehr and P. Schwintzer, Springer-Verlag Berlin, pp. 245–250.

Parker, R. L., 1994. *Geophysical Inverse Theory*. Princeton University Press, 386pp.

Parker, R. L., & Whaler, K. A. W., 1981. *Numerical methods for establishing solutions to the inverse problem of electromagnetic induction*. J. Geophys. Res., **86**, 9574–9584.

Parkinson, W. D., 1983. *Introduction to Geomagnetism*. Scottish Academic Press,. Edinburgh.

Reigber, Ch.; Lühr, H.; Schwintzer, P. , 2002. CHAMP mission status. *Advances in Space Research*, **30(2)**, 129–134.

Riedel, K., and A. Sidorenko, 1995. Minimum bias multiple taper spectral estimation. *IEEE Trans. on Signal Process.*, **43**, 188–195.

Roberts, R. G., 1984. The long period electromagnetic response of the Earth. *Geophys. J.R. astr. Soc.*, **78**, 547–572.

Rygaard-Hjalsted, C., C. G. Constable, and R. L. Parker, 1997. The influence of correlated crustal noise in modeling the main geomagnetic field. *Geophys. J. Int.*, **130**, 717–726.

Sabaka, T., N. Olsen & R.A. Langel, 2002. A comprehensive model of the near-Earth magnetic field: Phase 3. *Geophys. J. Int.*, **151**, 32–68.

Schultz, A. and J. C. Larsen, 1987. On the electrical conductivity of the mid-mantle: 1. Calculation of equivalent scalar magnetotelluric response functions. *Geophys. J.R. astr. Soc.*, **88**, 733–761.

Schultz, A. and J. C. Larsen, 1990. On the electrical conductivity of the mid-mantle: 2. Delineation of heterogeneity by application of extremal inverse solutions. *Geophys. J.R. astr. Soc.*, **101**, 565–580.

Shure, L., R. L. Parker and R. A. Langel, 1985. A preliminary harmonic spline model from Magsat data. *J. Geophys. Res.*, **90**, 11,505–11,512.

Tarits, P. & N. Grammatica , 2000. Electromagnetic induction effects by the solar quiet magnetic field at satellite altitude. *Geophys. Res. Lett.*, **27**, 4009–4012.

Tyler, R. H., S. Maus, & H. Lühr, 2003. Satellite Observations of magnetic fields due to ocean tidal flow. *Science*, **299**, 239–241.

Uyeshima, M., & A. Schultz, 2000. Geoelectromagnetic induction in a heterogeneous sphere: A new three-dimensional forward solver using a conservative staggered-grid finite difference method. *Geophys. J. Int.*, **140**, 635–650.

Velimsky, J., M. E. Everett, & Z. Martinec, 2003. The transient Dst induction signal at satellite altitudes for a realistic 3-D distribution of electrical conductivity in the crust and mantle. *Geophys. Res. Lett.*, **30**, art. no. 2002GL016671.

Weiss, C. J., & M. E. Everett, 1998. Geomagnetic induction in a heterogeneous sphere: fully three-dimensional test computations and the response of a realistic distribution of oceans and continents. *Geophys. J. Int.*, **135**, 650–662.

Xu, Y. S., Shankland, T. J., Poe, B. T., 2000. Laboratory-based electrical conductivity in the Earth's mantle. *J. Geophys. Res.*, **105**, 27865–27875.

C. G. Constable and S. C. Constable Institute of Geophysics and Planetary Physics, Scripps Institution of Oceanography, University of California at San Diego, La Jolla, Ca 92093-0225, USA. (e-mail: cconstable@ucsd.edu; sconstable@ucsd.edu)